Hindawi Publishing Corporation
Journal of Biomedicine and Biotechnology
Volume 2010, Article ID 134764, 9 pages
doi:10.1155/2010/134764

Research Article

Identification, Characterization, and Effects of *Xenopus laevis* PNAS-4 Gene on Embryonic Development

Fei Yan,[1,2,3] Xu-zhi Ruan,[1] Han-shuo Yang,[1] Shao-hua Yao,[1] Xin-yu Zhao,[1] Lan-tu Gou,[1] Fan-xin Ma,[1] Zhu Yuan,[1] Hong-xin Deng,[1] and Yu-quan Wei[1]

[1] *State Key Laboratory of Biotherapy and Cancer Center, West China Hospital, West China Medical School, Sichuan University, Chengdu 610041, China*
[2] *The Shenzhen Key Laboratory of Gene and Antibody Therapy, Center for Biotech and Bio-Medicine and Division of Life Sciences, Graduate School at Shenzhen, Tsinghua University, Shenzhen 518055, China*
[3] *Paul Lauterbur Center for Biomedical Imaging, Institute of Biomedical and Health Engineering, Shenzhen Institutes of Advanced Technology, Chinese Academy of Sciences, Shenzhen 518055, China*

Correspondence should be addressed to Hong-xin Deng, denghongx@yahoo.com.cn

Received 15 July 2009; Revised 1 November 2009; Accepted 1 March 2010

Academic Editor: Kenneth L. White

Apoptosis plays an important role in embryonic development. PNAS-4 has been demonstrated to induce apoptosis in several cancer cells. In this study, we cloned *Xenopus laevis* PNAS-4 (xPNAS-4), which is homologous to the human PNAS-4 gene. Bioinformatics analysis for PNAS-4 indicated that xPNAS-4 shared 87.6% identity with human PNAS-4 and 85.5% with mouse PNAS-4. The phylogenetic tree of PNAS-4 protein was also summarized. An analysis of cellular localization using an EGFP-fused protein demonstrated that xPNAS-4 was localized in the perinuclear region of the cytoplasm. RT-PCR analysis revealed that xPNAS-4, as a maternally expressed gene, was present in all stages of early embryo development. Whole-mount in situ hybridization showed that xPNAS-4 was mainly expressed in ectoderm and mesoderm. Furthermore, microinjection of xPNAS-4 mRNA in vivo caused developmental defects manifesting as a small eye phenotype in the *Xenopous* embryos, and as a small eye or one-eye phenotype in developing zebrafish embryos. In addition, embryos microinjected with xPNAS-4 antisense morpholino oligonucleotides (MOs) exhibited a failure of head development and shortened axis.

1. Introduction

Apoptosis, which protects organisms by removing potentially damaged cells and unnecessary cells after differentiation, is a widely occurring phenomenon in animal development [1]. Recently, reports about apoptosis during embryonic development in various model organisms have flourished. Apoptosis occurs in blastocyst cavitation and continues during gastrulation in mammal and chicken cells [2, 3]. Increased caspase-like activity and DNA fragmentation occurs in *Xenopus laevis* (*X. laevis*) embryos at the gastrula stage [4, 5]. Stress-induced apoptosis has also been characterized in zebrafish embryos [6]. Moreover, studies have revealed that apoptosis may contribute to development of a variety of organs such as brain, heart, lungs, and kidneys [7–10].

X. laevis is considered as one of the most important model organisms for studying vertebrate development and diseases. In contrast with mouse embryos, the large and robust *X. laevis* embryos are accessible in the stages during which most important decisions of development are taken so that a large variety of methodologies can be used to analyze the genetic regulation of many different developmental processes.

PNAS-4 was previously identified as a novel apoptosis-related protein in human acute promyelocytic leukemia NB4 cells. Recently, a report showed that the human PNAS-4 gene was activated during the early response to DNA damage [11]. In our previous studies, we proved that the overexpression of PNAS-4 induced cancer cell apoptosis via the activation of a mitochondrial pathway [12]. The potential antitumor effects of human PNAS-4 were also

demonstrated [13, 14]. To understand the biological function of the PNAS-4 gene in development, we first cloned the homologous PNAS-4 gene from *X. laevis* based on PNAS-4 bioinformatics analysis. In the present work, we addressed the preliminary functional annotation of *X. laevis* PNAS-4 (xPNAS-4) including protein sequence characterization, subcellular localization, gene expression profiles in developing embryos, and the impacts of microinjection of xPNAS-4 mRNA or antisense morpholino oligonucleotides (MOs) on embryonic development. Our primary studies on xPNAS-4 showed that xPNAS-4 may play important roles in embryo development.

2. Materials and Methods

2.1. Cell Lines and Animal Models. The HEK (Human embryonic kidney) 293 epithelial cell line was purchased from ATCC. Female *Xenopus laevis* were injected with 300–500 IU human chorionic gonadotropin (hCG) on the evening before egg collection. Nine to 12 hours after injection, eggs were collected and transferred into a fresh petri dish with culture medium. Staging of embryos was performed according to Nieuwkoop and Faber [15]. Zebrafish embryos were obtained and maintained as described in the zebrafish book [16].

2.2. Identification of xPNAS-4 cDNA and Plasmid Constructs. The *Xenopus* homolog of PNAS-4 (xPNAS-4) was identified in silico by blasting the *X. laevis* database with the full-length sequence of the human PNAS-4 protein (GenBank protein_id **NP_057160**). The cDNA of xPNAS-4 gene (GenBank accession no. **BC087412**) was amplified using the primer combination 5′-GGATCCATGGCCAACCAGCCCATCATC-3′ and 5′-CTCGAGCTATAGTTTTGTGTGGCGCCCAGG-3′. RT-PCR amplification was carried out in a MyCycler thermal cycler (Bio-Rad) using the following program: reverse transcription at 50°C for 40 minutes, and denaturing at 94°C for 2 minutes, followed by a standard touchdown PCR regime of 94°C for 30 seconds, 60°C for 30 seconds, and 72°C for 40 seconds (15 cycles, −1°C/cycle), and 94°C for 30 seconds, 48°C for 30 seconds, and 72°C for 40 seconds (35 cycles). The PCR product was cloned directly into the pGEM-T easy vector (Promega) to obtain pGEM-T-xPNAS-4 plasmid. DNA sequencing was performed by BigDye Terminator Cycle sequencing and the sequences were obtained with a 3730 DNA Analyzer (Applied Biosystems). In order to construct the pEGFP-N1-xPNAS-4 plasmid, the following primers were used, the sense primer: 5′-CCGCTCGAGATGGCCAACCAGCCCATCA-3′ and the antisense primer: 5′-CGGGATCCCGTAGTTTTGTGTGGCGCCCAG-3′, containing the *Xho* I and *Bam*H I restriction sites (underlined), respectively. The termination codon was removed to be in-frame with the enhanced green fluorescent protein (EGFP) sequence. The following amplification procedure was applied: initial PCR activation step at 94°C for 4 minutes, 35 PCR amplification cycles at 94°C for 30 seconds, 55°C for 30 seconds, 72°C for 40 seconds and a final extension cycle of 72°C for 10 minutes.

2.3. Bioinformatics. Nucleotide sequence and conserved domain analysis were carried out using BLAST programs (http://www.ncbi.nlm.nih.gov/blast/). Alignment of amino acid sequences was constructed using the Clustal W method (http://www.ebi.ac.uk/clustalw/) [17]. Homology analysis and molecular evolutionary analysis were generated using Lasergene Software and the MegAlign program (DNASTAR).

2.4. RT-PCR Analysis. Semiquantitative RT-PCR analysis of xPNAS-4 expression was performed using the above-mentioned primers. As an internal control for RNA quality, the housekeeping gene ornithine decarboxylase (ODC) was also amplified with sense primer 5′-GTCAATGATGGAGTGTATGGATC-3′ and antisense primer 5′-TCCATTCCGCTCTCCTGAGCAC-3′ according to published document [18]. Both reactions were amplified by using the same number of extension cycles (30 cycles). The samples were resolved on a 1.5% agarose gel with 1 μg/mL of ethidium bromide, and analyzed in a UV-Transilluminator mini darkroom using Quantity One Software (Bio-Rad).

2.5. In Situ RNA Hybridization. Whole-mount in situ hybridizations were performed according to the method of Harland [19]. Digoxigenin-rUTP-labeled antisense probes for xPNAS-4 were synthesized from pGEM-T-xPNAS-4 plasmid via Sp6 RNA polymerase. Hybridized transcripts were visualized in situ with antidigoxigenin antibodies and photographed using a Nikon dissecting microscope with an attached camera.

2.6. Cellular Localization. 5×10^5 HEK293 cells which had been grown in DMEM culture medium containing 10% FBS, 100 units/mL penicillin, and 100 mg/mL streptomycin were seeded on 6-well plates in a 37°C incubator with 5% CO_2. Transfections were performed according to the manufacturer's recommendations by using 10 μL of lipofectamine 2000 (Invitrogen) and either 4 μg of pEGFP-N1 or pEGFP-N1-xPNAS-4 plasmid DNA. The culture medium was changed after 6 hours with growth medium and maintained for another 24 hours to allow expression of the fusion protein. The transfected cells were examined under a Zeiss Axiophot fluorescence microscope.

2.7. In Vitro Transcription and Microinjection. Capped mRNAs used for microinjection in vitro were produced using an mMessage mMachine kit (Ambion). The reaction was set up in a total volume of 50 μL containing 2.5 μg *Xho* I—linearized pGEM-T-xPNAS-4 plasmid, 1×transcription buffer, 0.5 mM dNTPs, 2.5 mM RNA cap structure analogue, 10 mM DTT, 20 U RNAsin, and 40 U T7 RNA polymerase, and then incubated for 2 hours at 37°C. The templates were digested with 10 U of RNase free DNase I by incubating the samples for 30 minutes at 37°C. The volume was increased with RNase free water to 100 μL, and then the samples were applied on Quick spin columns (Ambion) to purify the products. *Xenopus* embryos at the one-cell stage were used for microinjection.

```
xPNAS-4  -MANQPIILNVYDMYWINEYTSSLGIGVFHSGIQVYGREFAYGGHPYPFS 49
hPNAS-4  MGANQLVVLNVYDMYWMNEYTSSIGIGVFHSGIEVYGREFAYGGHPYPFS 50
           *** ::********:******:*********:*****************

xPNAS-4  GVFEISPGDSTELGDTFKFKEAIALGSTDFTENDIEKIIEELGKEYKGNA 99
hPNAS-4  GIFEISPGNASELGETFKFKEAVVLGSTDFLEDDIEKIVEELGKEYKGNA 100
         *:*******:::***:********:.****** *:*****:***********

xPNAS-4  YHLMHKNCNHFSSALSEILCGKEIPRWVNRLAYFSTCVPFLQSCLPKEWL 149
hPNAS-4  YHLMHKNCNHFSSALSEILCGKEIPRWINRLAYFSSCIPFLQSCLPKEWL 150
         ****************************:********:*:************

xPNAS-4  TPAALQSSISQELQDELEEAEDAAASASTSTTAMP-RPGRHTKL 192
hPNAS-4  TPAALQSSVSQELQDELEEAEDAAASASVASTAAGSRPGRHTKL 194
         ********:********************.::**   ********
```

(a)

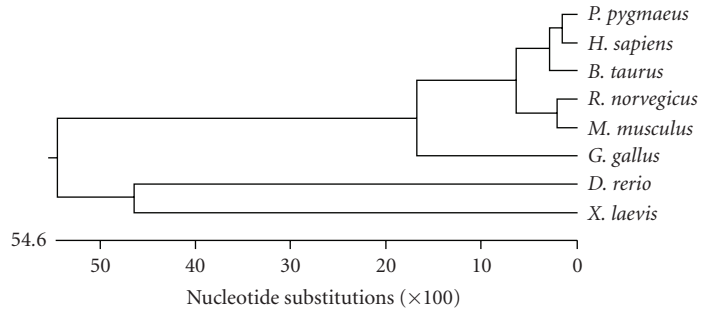

(b)

Figure 1: Comparison of the PNAS-4 protein sequence from *X. laevis* (GenBank protein_id: **AAH87412**) with those of other species. (a) Alignment of xPNAS-4 and hPNAS-4 protein sequences (GenBank protein_id: **NP_057160**) showing that they are homologous proteins. There is a DUF862 domain (underlined) in the hPNAS-4 and xPNAS-4 proteins. Asterisks (∗) indicate amino acid residues that are conserved across species. Colons (:) indicate strong similarity between protein xPNAS-4 and hPNAS-4. Dots (·) indicate weak similarity. (b) Phylogenetic tree of the PNAS-4 nucleotide sequences.

2.8. Whole-Mount TUNEL Staining. Published procedures for the whole-mount TUNEL staining of embryos were followed [20]. In brief, embryos were fixed overnight at 4°C in a 4% solution of formaldehyde in PBS. The samples were washed twice in 100 mM Tris-HCl buffer, pH 7.5, containing 150 mM sodium chloride and 0.1% Tween 20 (TBST), and fixed in methanol at −20°C for an additional 24 hours. The samples were washed three times at room temperature for 15 minutes in TBST to rehydrate the embryos following methanol fixation. The samples were transferred to TUNEL buffer (25 mM Tris-HCl, pH 6.6, containing 200 mM sodium cacodylate, 5 mM cobalt chloride, and 0.25% bovine serum albumin), and washed for 30 minutes. Fluorescent labeling of fragmented DNA in the samples was carried out for 1 hour at 37°C in TUNEL buffer containing 1 mM fluorescein-dUTP and 50 units/mL terminal deoxynucleotidyl transferase. The reaction was stopped by washing the sample in TBST buffer five times for 5 minutes at room temperature. The fluorescein-labeled TUNEL-positive cells were photographed using an Olympus microscope with excitation at 460–490 nm and emission at 510 nm.

2.9. Morpholino Oligonucleotides and Microinjections. All antisense morpholino oligonucleotides (MOs) were designed and supplied by Gene Tools Co. of America. MOs used in this study were as follows: xPNAS-4 MO (5′-TCTCCT-CCTCCTCCTGAGAATATCC-3′), and Control MO (5′-CCTCTTACCTCAGTTACAATTTATA-3′). Both xPNAS-4 MO and control MO were diluted to be 5 ng/nL and stored at −80°C in aliquots. Microinjection was performed in 1-MMR containing 5% ficoll (Sigma) solution. MOs were microinjected into the animal blastomere of stage-2 embryos. For rescue experiments, RNA and MOs were premixed. Co-injection was performed at two different ratios: 20 ng xPNAS-4 MO plus 450 pg xPNAS-4 mRNA and 20 ng xPNAS-4 MO plus 900 pg xPNAS-4 mRNA.

3. Results and Discussion

3.1. Bioinformatics. By blasting the *X. laevis* database with a human full-length PNAS-4 protein sequence (GenBank protein_id: **NP_057160**), we found an *X. laevis* PNAS-4 homologue (GenBank protein_id: **AAH87412**) which we named xPNAS-4. The xPNAS-4 cDNA sequence contains an open reading frame of 579 bp encoding 192 amino acids. Just like the human PNAS-4 protein, xPNAS-4 contains a putative DUF862 conserved domain corresponding to amino acid residues 4 to 131 (Figure 1(a)). The sequence of xPNAS-4 protein was compared with those of other species including *Bos Taurus* (GenBank protein_id. **XP_597874**),

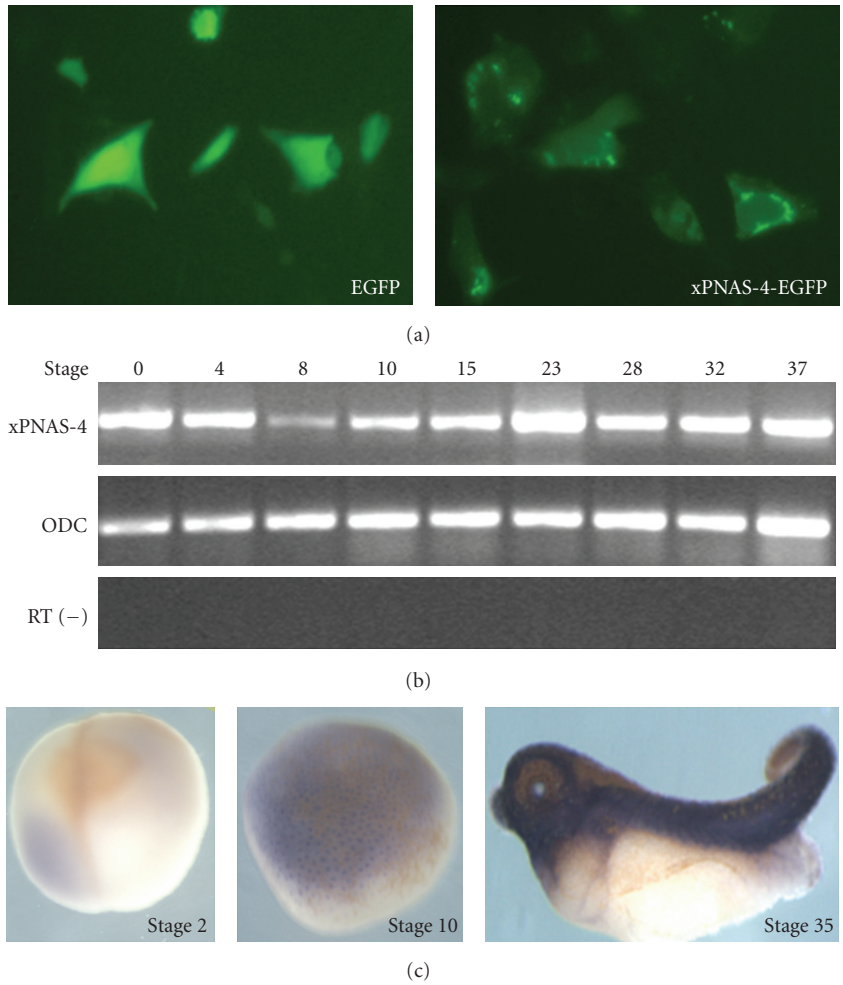

Figure 2: Cellular localization, and temporal and spatial expression patterns of xPNAS-4. (a) HEK293 cells were transfected with pEGFP-N1 or pEGFP-N1-xPNAS-4 plasmids as explained in materials and methods. Left: pEGFP-N1 transfected cells (200×); Right: pEGFP-N1-xPNAS-4 transfected cells (200×). (b) Analysis of the temporal expression pattern of xPNAS-4 gene by semiquantitative RT-PCR. ODC: *X. laevis* ornithine decarboxylase as internal control gene. RT (–): control reverse transcription without template. (c) Whole mount in situ hybridizations showing the spatial expression pattern of xPNAS-4 gene. The upper-left image shows the expression pattern of the xPNAS-4 gene in a stage-2 embryo. The upper-right image shows the expression pattern of the xPNAS-4 gene in a stage-10 embryo (beginning of gastrulation). An ubiquitous expression pattern (purple staining) can be seen. The lower image shows the expression pattern of the xPNAS-4 gene at stage 35. xPNAS-4 transcripts were present in the head, dorsal neural tissue, and prospective heart.

Pongo pygmaeus (GenBank protein_id: **Q5R456**), *Homo sapiens* (GenBank protein_id: **NP_057160**), *Gallus gallus* (GenBank protein_id: **NP_001008460**), *Danio rerio* (GenBank protein_id: **NP_001003532**), *Rattus norvegicus* (GenBank protein_id: **AAH83584**), and *Mus musculus* (GenBank protein_id: **Q9D291**), the identity was 88.1%, 87.6%, 87.6%, 87.0%, 86.0%, 85.5%, and 85.5%, respectively. This confirmed that these genes share a common ancestor. Based on the homology analysis, a phylogenetic tree of PNAS-4 proteins was constructed (Figure 1(b)).

3.2. Cellular Localization of xPNAS-4. To examine xPNAS-4 cellular localization, we fused xPNAS-4 to EGFP. Expression of xPNAS-4-EGFP in HEK293 cells appeared in the cytoplasm and was closely located around the nuclei, but the control (EGFP) protein was evenly distributed throughout the whole cell without any compartmentalization (Figure 2(a)). Thus, xPNAS-4 was a cytoplasmic protein which was localized in the perinuclear region of the cytoplasm.

3.3. Temporal and Spatial Expression of xPNAS-4 in X. Laevis Embryos. In order to determine the temporal expression pattern of xPNAS-4, the mRNA level at different developmental stages was detected. Semiquantitative RT-PCR analysis showed that xPNAS-4 mRNA could be detected at all stages of development, from the unfertilized egg to the tadpole stage (Figure 2(b)). The lowest expression level of xPNAS-4 appeared at stage 8 (the mid-blastula transition). Before the mid-blastula transition, the expression level of xPNAS-4 decreased along with the rate of cell division. After the mid-blastula transition, however, the expression level of xPNAS-4 increased rapidly. This result suggests that

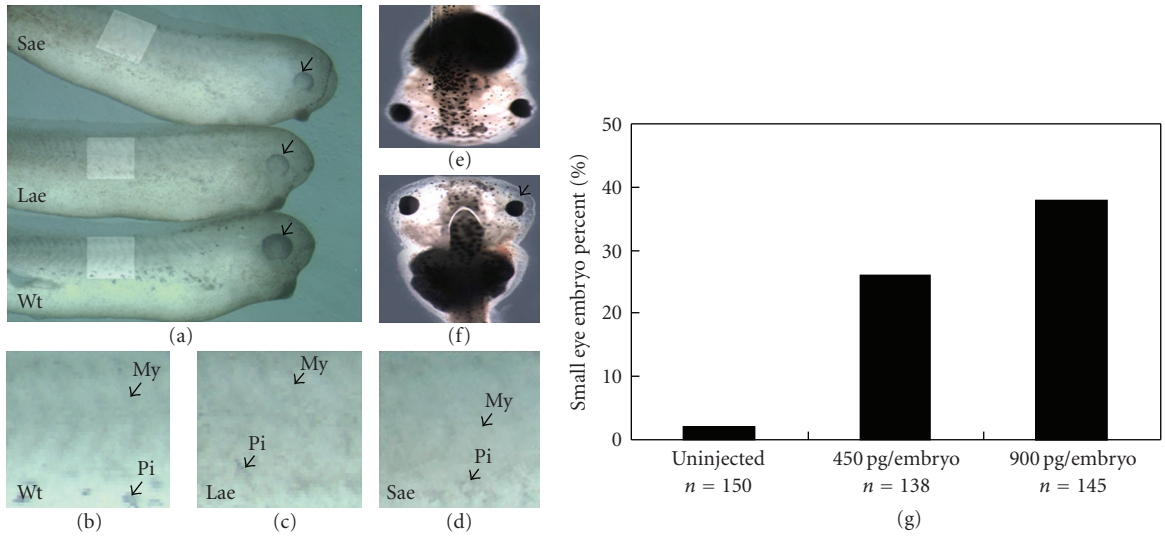

Figure 3: Developmental defects in *Xenopus* embryos caused by microinjection of xPNAS-4. Embryos were injected once into the dorsal marginal zone at the one-cell stage with 450 pg or 900 pg of xPNAS-4 mRNA. (a) Lateral view of stage 35 tadpoles showing (bottom to top) an unaffected embryo (Wt, bottom); a mildly affected embryo (Lae, middle) and a strongly affected embryo (Sae, upper). Arrows indicate embryos' eyes. (b), (c), and (d) are magnified views from local regions in the pictures. Abbreviations: Wt, wild type; Lae, mildly affected embryo; Sae, strongly affected embryo; My, myotome; Pi, pigment. (e) Dorsal view of an uninjected stage 43 embryo. (f) Dorsal view of stage 43 embryo which was injected with 900 pg of xPNAS-4 mRNA. (g) Graphical representation of the percent of embryos injected with xPNAS-4 mRNA with the small eye phenotype at stage 35 (n = the number of embryos in each group).

there is xPNAS-4 message of maternal origin, since zygotic transcription starts at the mid-blastula transition (MBT) [21]. Indeed, many other apoptosis-related genes showed similar transcription patterns [22, 23]. Consequently, xPNAS-4 may play an important role in *Xenopus* embryo development.

For a better understanding of the expression of xPNAS-4 mRNA in embryonic tissues, whole mount in situ hybridization was performed. Figure 2(c) shows that xPNAS-4 was mainly present along ectoderm and mesoderm. The expression of xPNAS-4 could be detected at stage 2. This was consistent with the result of semiquantitative RT-PCR. Up to the gastrula stage (stage 10), the expression of xPNAS-4 was present ubiquitously in the embryo. By the tail bud stage (stage 35), the expression of xPNAS-4 mainly appeared in the head and dorsal neural tissue. Furthermore, a weak expression of xPNAS-4 could also be observed in the prospective heart of the tail bud embryo. Thus, xPNAS-4 is a maternally expressed gene. Its transcripts are present ubiquitously in gastrula stage embryos, while tissue specific expression can be detected in later embryogenesis.

3.4. Microinjections of xPNAS-4 mRNA Caused Developmental Defects. To explore the role of xPNAS-4 during embryonic development, the synthesized xPNAS-4 mRNA was injected into *Xenopus* embryos at the one-cell stage. As shown in Figures 3(a), 3(e), and 3(f), the eyes were poorly developed and were smaller than normal. Some embryos also showed defective myotomes and reduced pigmentation (Figures 3(b)–3(d)). The abnormal eye phenotype was dose dependent. About 26% small eye embryos were produced by injection of xPNAS-4 mRNA at 450 pg/embryo; while about 38% small eye embryos were observed when xPNAS-4 mRNA was injected at 900 pg/embryo. The uninjected embryos only produced 2% eye abnormalities (Figure 3(g)). This result demonstrated that xPNAS-4 plays an important role in embryonic eye development.

Taking into consideration the high conservation of xPNAS-4 protein with that of zebrafish, we hypothesized that xPNAS-4 would act in a similar manner in zebrafish, another developmental system used to study eye development [24]. To test this postulation, we injected xPNAS-4 mRNA into zebrafish embryos at the one-cell stage. The resulting phenotype was quite similar to what occurred with xPNAS-4 mRNA injection in *Xenopus*. Following injection of 300 pg xPNAS-4 mRNA 38% of embryos had abnormal eyes, and after injection of 600 pg mRNA 86% of embryos exhibited abnormal eye development. Unlike *Xenopus* embryos, however, zebrafish embryos with eye defects could be divided into two groups: the less affected embryos had reduced eye size, while the more strongly affected embryos exhibited a one-eye phenotype (Figures 4(d), 4(e), and 4(h)). In addition to the eye defect, some strongly affected embryos had a bent axis (Figures 4(f) and 4(i)). Similarly, the defects produced by heterologous expression of xPNAS-4 were also dose dependent. Injection of 300 pg of xPNAS-4 mRNA resulted in 34% reduced eye embryos and 4% one-eye embryos, while injection of 600 pg of xPNAS-4 mRNA resulted in 24% reduced eye embryos and 62% one-eye embryos (Figures 4(j)–4(l)). All of the uninjected embryos were normal (Figures 4(a)–4(c), and 4(g)).

3.5. xPNAS-4 Induces Eye Developmental Defects Via Apoptosis. To confirm that the developmental defects caused

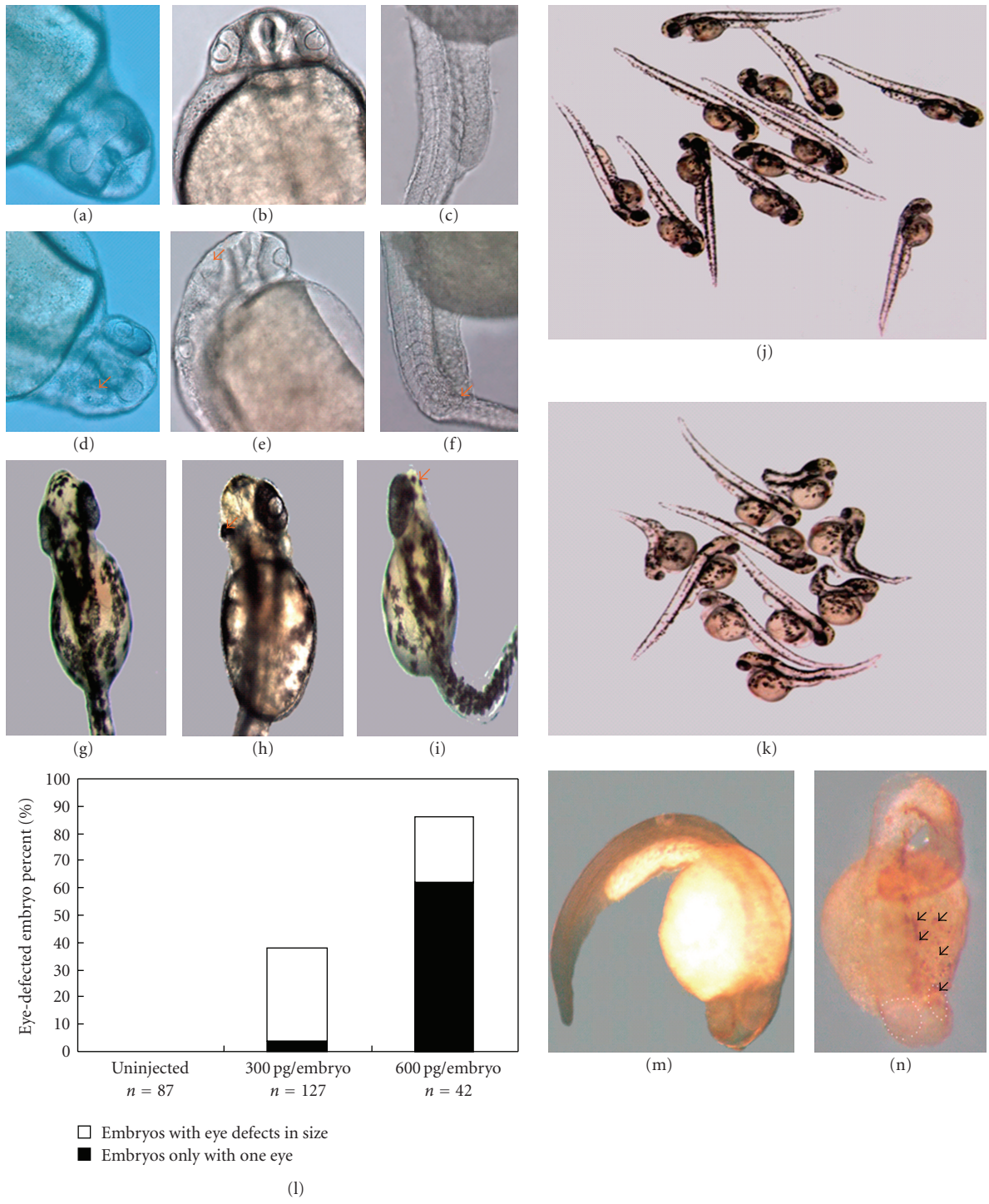

Figure 4: Heterologous expression of xPNAS-4 causes eye defects in zebrafish embryos. Embryos were injected at the one-cell stage with 300 pg or 600 pg of xPNAS-4 mRNA. Figures 4(a)–4(f) show embryos at 24 hours post fertilization (hpf). (a) Ventral view of a wild type zebrafish embryo with anterior to the bottom right. (b) Ventral view of a wild type zebrafish embryo with anterior to the top. (c) Lateral view of the normal axis of a wild type embryo. (d) Ventral view of a reduced-eye embryo. Arrow indicates the reduced eye. (e) Ventral view of a one-eyed embryo with anterior to the top. Arrow indicates the lost eye. (f) Lateral view of bent axis defects (arrow) of xPNAS-4 mRNA injected embryo. Figures 4(g)–4(i) show embryos at 48 hpf with anterior to the top. (g) Dorsal view of a wild type zebrafish embryo. (h) Dorsal view of an embryo with a reduced size eye. (i) Dorsal view of a one-eyed embryo. (j) Population of wild type zebrafish embryos at 48 hpf. (k) Population of zebrafish embryos with eye defects at 48 hpf. (l) Quantitative data for eye defects in injected and uninjected zebrafish embryos at 48 hpf. *N* is the number of embryos examined for each treatment. (m) Whole-mount TUNEL staining of a wild type embryo at 24 hpf. (n) Whole-mount TUNEL staining of an embryo with an eye defect at 24 hpf. A high number of TUNEL-positive cells were detected on the side of injection (black arrow). Dotted circle indicates the developing eyes.

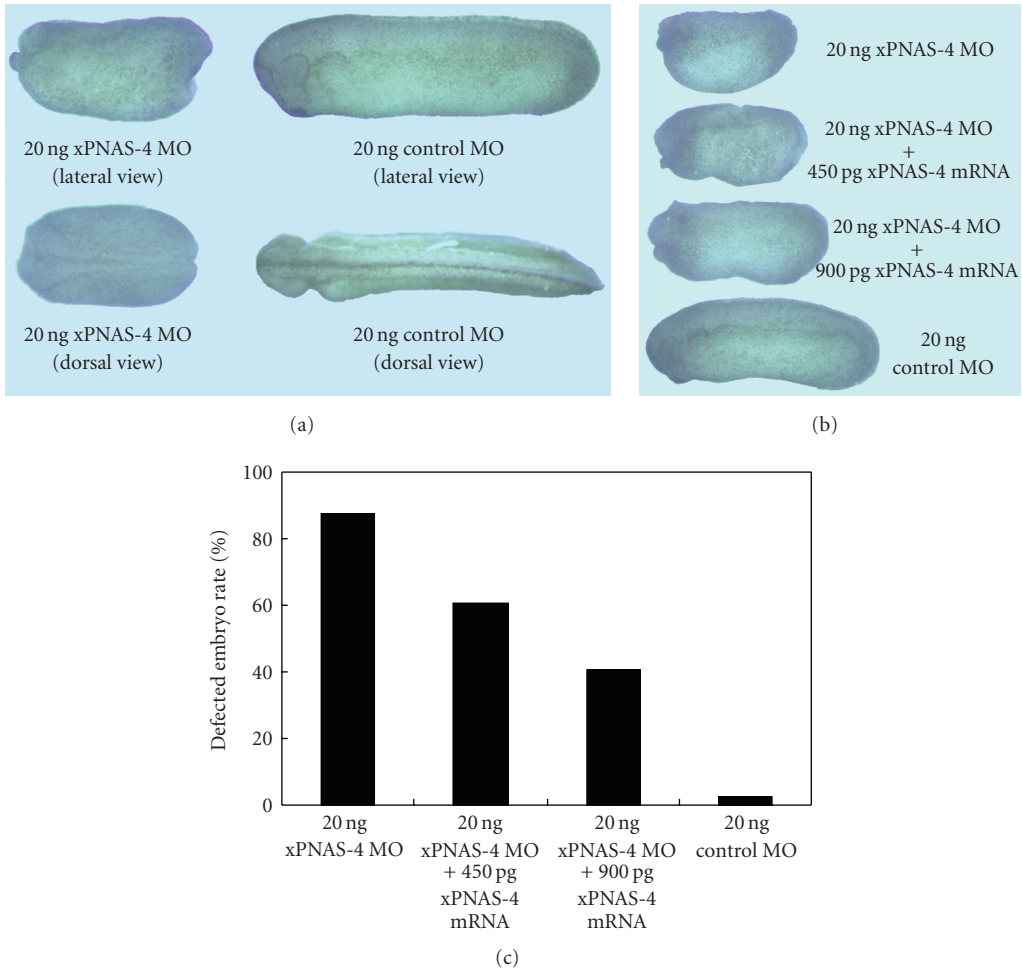

Figure 5: Effect of xPNAS-4 MOs microinjection. (a) Embryos microinjected with 20 ng of xPNAS-4 MO exhibited failure of head development and shortened axis defects (left), but embryos microinjected with 20 ng of control MO embryos were normal (right). (b) The embryos were partially rescued by co-injected with 450 pg of xPNAS-4 mRNA and 20 ng of xPNAS-4 MO (the second row) in comparison with embryos microinjected with 20 ng of xPNAS-4 MO alone (the first row). Better rescue was observed after co-injection of 20 ng of xPNAS-4 MO plus 900 pg of xPNAS-4 mRNA (the third row). The fourth row shows a normal embryo microinjected with 20 ng of control MO. (c) The rate of defective embryos seen in the experiment.

by heterologous injection of xPNAS-4 resulted from apoptosis, whole-mount TUNEL (terminal deoxynucleotidyl transferase-mediated nicked-end labeling) staining, a highly sensitive indicator of DNA fragmentation in situ was employed to detect the presence of apoptotic cells. TUNEL-positive cells were present at high frequency on the side of zebrafish embryos on which eye development was affected (Figure 4(n)) when compared with the control embryos (Figure 4(m)).

It is widely accepted that apoptosis is involved in many embryological processes and plays a significant role in animal development. If apoptosis is disturbed, tissues develop abnormally and various syndromes or cancers develop [25]. The tumor suppressor protein p53, a widely known trigger of apoptosis, has been implicated as an important protein in embryonic development. Inappropriate overexpression or underexpression of p53 can lead to embryonic lethality or increased risk of malformations [26]. Furthermore, an effect of apoptosis on eye development has also well been documented. Inactivation of p53 function by gene knock-out [27] or through lens specific promoter-driven expression of the viral gene E6, interrupts normal apoptosis in the lens leading to formation of a cataract [28, 29]. The caspase family including caspase-1, -2, -3, -4, -6, and -9, is involved in eye differentiation in different species of vertebrates [30]. During development of the chicken lens, members of the Bcl-2 family, such as Bcl-2, Bax, Bad, and Bcl-Xs/l, are abundantly expressed between stages E12 and E16 [31]. In our experiment, we found a considerable number of apoptotic cells appeared in abnormal embryos by whole mount in situ hybridization, suggesting that abnormal eye development resulted from the overexpression or heterologous expression of xPNAS-4. This further confirmed that xPNAS-4 is involved in apoptosis during embryonic development.

3.6. Depletion of xPNAS-4 Affects the Normal Process of Embryos. To further define the function of xPNAS-4 during embryogenesis, we performed translational inhibition of xPNAS-4 by microinjecting antisense morpholino oligonucleotides (MOs). Control and xPNAS-4 MOs (20 ng) were microinjected into the animal blastomere of stage-2 embryos. As development proceeded, 86.7% of embryos ($n = 98$) microinjected with xPNAS-4 MO had a failure of head development and a shortened axis (Figures 5(a) and 5(c)). All embryos which had a failure of head development exhibited a shortened axis. Embryos with failed head development died in the late tailbud stage, while control MO microinjected embryos (98.4%, $n = 128$) developed to the next stages normally.

In order to confirm that the phenotypes were due to translational inhibition of xPNAS-4, we co-injected xPNAS-4 MO and in vitro transcribed capped xPNAS-4 mRNA. As expected, the failure of head development and the shortened axis were rescued to some extent after co-injection of 20 ng xPNAS-4 MO plus 450 pg xPNAS-4 mRNA. About 56.5% of embryos ($n = 92$) exhibited a failure of head development. The defective embryos had longer axes than those microinjected with xPNAS-4 MO alone. A greater extent of rescue was observed after co-injection of 20 ng xPNAS-4 MO plus 900 pg xPNAS-4 mRNA. Only 32.1% embryos ($n = 78$) showed the failure of head development. The defective embryos had longer axes than those microinjected with xPNAS-4 MO plus 450 pg xPNAS-4 mRNA (Figures 5(b) and 5(c)). These results revealed that the failure of head development and shortened axis caused by xPNAS-4 MO microinjection were due to depletion of xPNAS-4.

We also found similar defects using zebrafish as a model system in our previous studies. Loss of function of the PNAS-4 gene caused gastrulation defects with a shorter and broader axis, as well as a posteriorly mis-positioned prechordal plate, due to the defective convergence and extension movement [32]. In the present work, we found that loss of function of the PNAS-4 gene in *X. laevis* embryos resulted in the failure of head development and a shortened axis. The phenotypic differences were probably due to the different species or differences in the inhibition rate of morpholino oligonucleotides.

4. Conclusion

PNAS-4 protein is well conserved across species. Here we identified the PNAS-4 homolog from *X. laevis* based on the amino acid sequence of human PNAS-4 protein. The xPNAS-4 protein is very similar to human PNAS-4. The high similarity suggested that the human and *X. laevis* proteins might have analogous functions. Cellular localization suggested that xPNAS-4 is in the cytoplasm and is located around the nucleus. We also proved that xPNAS-4 is a maternally expressed gene. Investigation of the developmental expression pattern showed that xPNAS-4 is present throughout embryogenesis and undergoes pronounced changes in its level of mRNA during embryo development. In addition, microinjections of xPNAS-4 mRNA into *Xenopus laevis* embryos resulted in embryonic developmental defects including a small eye phenotype in developing *X. laevis* embryos, and a reduced eye size or one-eye phenotype in the developing zebrafish embryos. Whole mount in situ hybridization further confirmed that the developmental defects resulted from apoptosis during embryonic development. Furthermore, embryos microinjected with xPNAS-4 MO had a failure of head development and shortened axis.

In conclusion, our results provide important clues about the molecular mechanisms by which xPNAS-4 regulates developmental processes.

Acknowledgments

This work was supported by grants from the National Basic Research Program of China (2004CB51880) and grants from the National Natural Science Foundation of China (no. 30900749).

References

[1] M. D. Jacobson, M. Weil, and M. C. Raff, "Programmed cell death in animal development," *Cell*, vol. 88, no. 3, pp. 347–354, 1997.

[2] E. Coucouvanis and G. R. Martin, "Signals for death and survival: a two-step mechanism for cavitation in the vertebrate embryo," *Cell*, vol. 83, no. 2, pp. 279–287, 1995.

[3] E. J. Sanders and E. Parker, "The role of mitochondria, cytochrome c and caspases-9 in embryonic lens fibre cell denucleation," *Journal of Anatomy*, vol. 201, no. 2, pp. 121–135, 2002.

[4] K. Nakajima, A. Takahashi, and Y. Yaoita, "Structure, expression, and function of the *Xenopus laevis* caspase family," *Journal of Biological Chemistry*, vol. 275, no. 14, pp. 10484–10491, 2000.

[5] C. Hensey and J. Gautier, "A developmental timer that regulates apoptosis at the onset of gastrulation," *Mechanisms of Development*, vol. 69, no. 1-2, pp. 183–195, 1997.

[6] T. Yabu, S. Kishi, T. Okazaki, and M. Yamashita, "Characterization of zebrafish caspase-3 and induction of apoptosis through ceramide generation in fish fathead minnow tailbud cells and zebrafish embryo," *Biochemical Journal*, vol. 360, no. 1, pp. 39–47, 2001.

[7] K. A. Roth and C. D'Sa, "Apoptosis and brain development," *Mental Retardation and Developmental Disabilities Research Reviews*, vol. 7, no. 4, pp. 261–266, 2001.

[8] R. E. Poelmann, D. Molin, L. J. Wisse, and A. C. Gittenberger-de Groot, "Apoptosis in cardiac development," *Cell and Tissue Research*, vol. 301, no. 1, pp. 43–52, 2000.

[9] L. M. Scavo, R. Ertsey, C. J. Chapin, L. Allen, and J. A. Kitterman, "Apoptosis in the development of rat and human fetal lungs," *American Journal of Respiratory Cell and Molecular Biology*, vol. 18, no. 1, pp. 21–31, 1998.

[10] J. Savill, "Apoptosis and the kidney," *Journal of the American Society of Nephrology*, vol. 5, no. 1, pp. 12–21, 1994.

[11] V. Filippov, M. Filippova, D. Sinha, et al., "PNAS-4: a novel pro-apoptotic gene activated during the early response to DNA damage," *Proceedings of the American Association for Cancer Research*, vol. 46, p. 717, 2005.

[12] F. Yan, L. Gou, J. Yang, et al., "A novel pro-apoptosis gene PNAS4 that induces apoptosis in A549 human lung adenocarcinoma cells and inhibits tumor growth in mice," *Biochimie*, vol. 91, no. 4, pp. 502–507, 2009.

[13] F. Yang, Z. Li, H. Deng, et al., "Efficient inhibition of ovarian cancer growth and prolonged survival by transfection with a novel pro-apoptotic gene, hPNAS-4, in a mouse model: in vivo and in vitro results," *Oncology*, vol. 75, no. 3-4, pp. 137–144, 2008.

[14] S. Hou, Z. Zhao, F. Yan, et al., "Genetic transfer of PNAS-4 induces apoptosis and enhances sensitivity to gemcitabine in lung cancer," *Cell Biology International*, vol. 33, no. 3, pp. 276–282, 2009.

[15] P. D. Nieuwkoop and J. Faber, *Normal Table of Xenopus laevis (Daudin)*, Garland Publishing, New York, NY, USA, 1994.

[16] M. Westerfield, *The Zebrafish Book*, University of Oregon, Eugene, Ore, USA, 3rd edition, 1995.

[17] C. B. Thompson, "Apoptosis in the pathogenesis and treatment of disease," *Science*, vol. 267, no. 5203, pp. 1456–1462, 1995.

[18] T. Bassez, J. Paris, F. Omilli, C. Dorel, and H. B. Osborne, "Post-transcriptional regulation of ornithine decarboxylase in *Xenopus laevis* oocytes," *Development*, vol. 110, no. 3, pp. 955–962, 1990.

[19] R. M. Harland, "In situ hybridization: an improved whole-mount method for *Xenopus* embryos," *Methods in Cell Biology*, vol. 36, pp. 685–695, 1991.

[20] T. Yabu, S. Todoriki, and M. Yamashita, "Stress-induced apoptosis by heat shock, UV and γ-ray irradiation in zebrafish embryos detected by increased caspase activity and whole-mount TUNEL staining," *Fisheries Science*, vol. 67, no. 2, pp. 333–340, 2001.

[21] J. Newport and M. Kirschner, "A major developmental transition in early *Xenopus* embryos: I. Characterization and timing of cellular changes at the midblastula stage," *Cell*, vol. 30, no. 3, pp. 675–686, 1982.

[22] M. Kai, T. Higo, J. Yokoska, et al., "Overexpression of S-adenosylmethionine decarboxylase (SAMDC) activates the maternal program of apoptosis shortly after MBT in *Xenopus* embryos," *International Journal of Developmental Biology*, vol. 44, no. 5, pp. 507–510, 2000.

[23] A. D. Carter and J. C. Sible, "Loss of XChk1 function triggers apoptosis after the midblastula transition in *Xenopus laevis* embryos," *Mechanisms of Development*, vol. 120, no. 3, pp. 315–323, 2003.

[24] A. S. Glass and R. Dahm, "The zebrafish as a model organism for eye development," *Ophthalmic Research*, vol. 36, no. 1, pp. 4–24, 2004.

[25] C. B. Thompson, "Apoptosis in the pathogenesis and treatment of disease," *Science*, vol. 267, no. 5203, pp. 1456–1462, 1995.

[26] J. Choi and L. A. Donehower, "p53 in embryonic development: maintaining a fine balance," *Cellular and Molecular Life Sciences*, vol. 55, no. 1, pp. 38–47, 1999.

[27] L. A. Donehower, M. Harvey, B. L. Slagle, et al., "Mice deficient for p53 are developmentally normal but susceptible to spontaneous tumours," *Nature*, vol. 356, no. 6366, pp. 215–221, 1992.

[28] H. Pan and A. E. Griep, "Altered cell cycle regulation in the lens of HPV-16 E6 or E7 transgenic mice: implications for tumor suppressor gene function in development," *Genes and Development*, vol. 8, no. 11, pp. 1285–1299, 1994.

[29] M. B. Reichel, R. R. Ali, F. D'Esposito, et al., "High frequency of persistent hyperplastic primary vitreous and cataracts in p53-deficient mice," *Cell Death and Differentiation*, vol. 5, no. 2, pp. 156–162, 1998.

[30] G. F. Weber and A. S. Menko, "The canonical intrinsic mitochondrial death pathway has a non-apoptotic role in signaling lens cell differentiation," *Journal of Biological Chemistry*, vol. 280, no. 23, pp. 22135–22145, 2005.

[31] M. A. Wride, E. Parker, and E. J. Sanders, "Members of the Bcl-2 and caspase families regulate nuclear degeneration during chick lens fibre differentiation," *Developmental Biology*, vol. 213, no. 1, pp. 142–156, 1999.

[32] S. Yao, L. Xie, M. Qian, et al., "Pnas4 is a novel regulator for convergence and extension during vertebrate gastrulation," *FEBS Letters*, vol. 582, no. 15, pp. 2325–2332, 2008.